International Conference on Applied Energy 2019
Aug 12-15, 2019, Västerås, Sweden
Paper ID: #438

OPTIMAL COST EVALUATION OF STAND-ALONE MICROGRIDS WITH DIFFERENT DESIGN

Xue Kong[1], Nan Li[1], Hailin Mu[1*], Hongye Wang[1]

1 Key Laboratory of Ocean Energy Utilization and Energy Conservation of Ministry of Education, Dalian University of Technology, Dalian 116024, China

ABSTRACT

In the resent years, microgrid has been widely used in the world and become a good solution to the urgent energy and environment issues. However, the high cost of microgrid limits the development of microgrid. In this paper, a novel design is presented to be compared with traditional design using a contrastive framework with renewable energy considering battery lifetime and renewable energy penetration. Numerical results show that the LCOE of the novel design can be reduced by 6.23% compared with traditional design.

Keywords: microgrid, energy storage system, gas turbine, LCOE

NONMENCLATURE

Nomenclature	
Indices	
n	time period index
t	time period index
Constants	
α	power-law exponent.
a_1, a_2, a_3, a_4, a_5	coefficient of battery life cycle curve.
b_1, b_2, b_3, b_4	coefficient of gas turbine efficiency curve.
k	power temperature coefficient.
R_{rated}	rated solar radiation in standard condition (W/m^2).
T_{rated}	rated temperature in standard condition (℃).
Parameters	
β	ratio of actual power used to available power in renewable energy system.
γ	Proportion of unmet load.
$\eta_{ESS\text{-}charge}$, $\eta_{ESS\text{-}disc}$	charging/discharging efficiency of batteries.
f(t)	load rate of gas turbine at time t.
$\eta_{GT}(t)$	efficiency of gas turbine at time t.
c_1, c_2	capital and loans as a percentage of total investment.
C_{ng}	natural gas price ($/kWh).
DOD	depth of discharge of lead-acid batteries.
f	inflation rate.
n_{ESS}	number of batteries.
$N_{cycles}(D_N)$	Cycle times of lead-acid battery under DOD D_N.
n_{PV}	number of photovoltaic panels.
n_{WT}	number of wind turbines.
$P_{ESS\text{-}change,\ max}$, $P_{ESS\text{-}disc,\ max}$	maximum rating charging/discharging power of battery storage at time t (kW).
$P_{PV}(t)$	available power from photovoltaic panels at time t (kW).
$P_{WT}(t)$	available power from wind-turbines at time t (kW).
$P_{PV\text{-}rated}$	rated power of photovoltaic panels in standard condition (kW).
$P_{WT\text{-}rated}$	rated power of wind turbine (kW).
r	actual discount rate.
r′	nominal discount rate.
R(t)	solar irradiance at time t (W/m^2).
T(t)	ambient temperature at time t (℃).

Selection and peer-review under responsibility of the scientific committee of the 11th Int. Conf. on Applied Energy (ICAE2019).

$v(t)$	wind speed at projected height at time t (m/s).
v_{rated}, v_{ci}, v_{co}	rated, cut-in and cut-out wind speeds of wind turbine (m/s).
$V_{ref}(t)$	wind speed at reference height at time t (m/s).
y	annual loan repayment ratio.
Z	height of wind turbine (m).
Z_{ref}	reference height of wind turbine (m).
Variables	
C_{cap}	total capital costs ($).
$C_{cap-ESS}$	capital cost of battery ($).
$CC_{cap-ESS}$	battery cost ($/kWh).
C_{fuel}	fuel cost ($).
$C_{o\&m}$	total operation and maintenance costs ($).
$C_{o\&m-WT}$, $C_{o\&m-PV}$, $C_{o\&m-ESS}$	WT/PV/ESS operation and maintenance costs ($).
$C_{rep-ESS}$	replacement cost of battery ($).
$E_{ESS}(t)$	battery capacity at time t (kWh)
$E_{ESS, max}$	rated battery capacity (kWh).
$F_{ng}(t)$	natural gas consumption at time t (kWh).
$F_{ng-total}$	total natural gas consumption (kWh).
$F_{ng-total}$	total natural gas consumption (kWh).
Load(t)	load considering at time t (kW).
$P_{ESS-charge}(t)$, $P_{ESS-disc}(t)$	charging/discharging power of battery storage at time t (kW).
$P_{GT}(t)$	power from gas turbine at time t (kW).
$P_{GT-rated}$	rated power of gas turbine (kW).
$P_{PV-real}(t)$	actual power from photovoltaic panels at time t (kW).
$P_{WT-real}(t)$	actual power from wind-turbines at time t (kW).

1. INTRODUCTION

In the current power system, as a result of resource endowment, China has developed a country where fossil fuel power generation is the main power generation mode. However, the problem of energy exhaustion and environmental pollution caused by traditional fossil energy power generation cannot be ignored definitely and needs to be addressed urgently. It was widely accepted that microgrid is a new power generation method due to its potential benefits to provide sustainable, environmentally friendly, and efficient electricity from renewable energy sources[1].

Microgrid contains renewable energy power generation units, such as wind turbine (WT), photovoltaic panels (PV) etc. has become a popular way to generate electricity [2-4]. At the same time, energy storage systems (ESS) become the default option to reduce the impact of renewable power generation uncertainty on power supply caused by the variability of the climate. As the result of the application of energy storage, the cost of generating electricity from microgrid is higher [5]. At present, most scholars exploring the optimization of energy storage system cost established cost-optimal microgrid model [6-9]. However, the impact of different microgrid designs on the generation cost is lesser. Therefore, the influence of two different microgrid designs on generation cost is preliminarily explored in this paper.

A novel design which contains WT, PV and gas turbine (GT) presented in this paper is compared with traditional microgrid design including WT, PV and ESS. In order to compare two different design methods of microgrid, the concept of Levelized Cost of electricity is used. Furthermore, we investigated the impact of battery life and renewable energy coupling rate on the comparative results.

2. METHODOLOGY

2.1. Model structures and assumption

2.1.1. Renewable energy

We assume that renewable resource generation consisting of WT and PV is determinate.

(1) Wind turbine

The output power of wind turbine is modelled using the piecewise function as a three-block [10] which is captured in (1).

$$P_{WT}(t)=\begin{cases} 0 & v(t)\le v_{ci}, v(t)\ge v_{co} \\ n_{WT}P_{WT\text{-}rated}\dfrac{v(t)-v_{ci}}{v_{rated}-v_{ci}} & v_{ci}<v(t)\le v_{rated} \\ n_{WT}P_{WT\text{-}rated} & v_{rated}<v(t)<v_{co} \end{cases} \quad (1)$$

The power from wind turbine is only related to the wind speed at projected height. Therefore, we need to carry out wind speed conversion according to the method mentioned in [11]. As shown in equation (2).

$$v(t)=v_{ref}(t)\left(\frac{Z}{Z_{ref}}\right)^{\alpha} \quad (2)$$

(2) Photovoltaic panels

The power from PV can be calculated by (3) at any time and the amount of photovoltaic output power is directly determined by solar irradiation and ambient temperature.

$$P_{PV}(t) = n_{PV} P_{PV\text{-}rated} \left(\frac{R(t)}{R_{rated}} \right) \left[1 + k\left(T(t) - T_{rated} \right) \right] \quad (3)$$

The power is acquired directly by solar irradiation and temperature under the standard conditions when the solar irradiation and temperature are equal to 1000W/m^2 and 25 ℃, respectively. Where k is temperature coefficient that values -0.0045.

2.1.2. Energy storage system

The energy dynamic model for lead-acid battery is presented in (4) for any given time.

$$E_{ESS}(t+1) = E_{ESS}(t) + \left(\eta_{ESS\text{-}charge} P_{ESS\text{-}charge}(t) - \frac{P_{ESS\text{-}disc}(t)}{\eta_{ESS\text{-}disc}} \right) \quad (4)$$

Where the battery efficiency during the charging and discharging processes are 0.85 and 0.98 respectively at any time.

The lifetime of the lead-acid battery which normally values around 4000 cycles is basically determined by its depth of the discharge(DOD)[12], as illustrated in Fig. 1.

The relation of cycle index and depth of discharge is calculated via formula (5).

$$N_{cycles} = a_1 + a_2 e^{a_3 \cdot D_N} + a_4 e^{a_5 \cdot D_N} \quad (5)$$

Where a_1, a_2, a_3, a_4 and a_5 are equal to be 0, 7753, -7.263, 2603 and -0.8455[2] respectively[13].

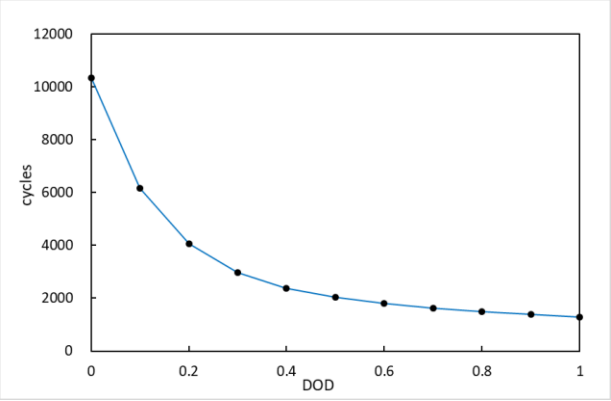

Fig 1 The relation of cycle index and depth of discharge of lead-acid batteries

2.1.3. Gas turbine

The efficiency curve which is widely used in CCHP systems [14-16] is employed to describe the dynamic model for the relationship between efficiency and load rate of the GT, as shown in (6). The load rate is given in (7). Where b_1, b_2, b_3 and b_4 are equal to be 0.1283, -0.6592, 0.7945 and 0.003 respectively [15]. It's worth mentioning that we make the following assumptions that equipment capacity is continuously distributed, there is no start and stop time limit for GT and the equipment always operates reliably.

The nature gas consumption determined by fitting load rate and efficiency curve of the GT, as illustrated in Fig. 2.

$$\eta_{GT}(t) = b_1 f(t)^3 + b_2 f(t)^2 + b_3 f(t) + b_4 \quad (6)$$

$$f(t) = \frac{P_{GT}(t)}{P_{GT\text{-}rated}} \quad (7)$$

$$F_{ng}(t) = \frac{P_{GT}(t)}{\eta_{GT}(t)} \quad (8)$$

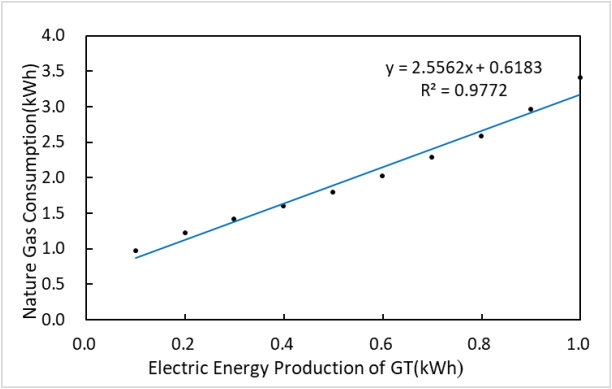

Fig 2 gas consumption curve of GT

2.2. Problem formulation

2.2.1. Objective function

Two different designs of microgrid are considered in this section. The operating cost is optimized in the objective function which takes into account the impact of the battery operating state on the battery life in the first design. The optimal daily operating cost includes operation and maintenance cost of WT, PV and lead-acid battery, daily cost of capital and daily cost of replacement cost of batteries. which is presented in the equation (9)-(14). The initial investment and loan are taken into account by the capital cost of batteries. Constrains (12) is the capital recovery cost (a ratio used to calculate the present value of an annuity) [17]. Furthermore, the impact of inflation on investment costs is also taken into account which is calculated by (13). It is worth mentioning that the

replacement cost of the battery is thought to vary with inflation.

The optimal daily operating cost includes daily operation and maintenance cost of WT, PV and GT, daily fuel consumption cost which is given as (15)-(17).

Design1:

$$\min \ C_{o\&m} + C_{cap\text{-}ESS} + C_{rep\text{-}ESS} \tag{9}$$

$$C_{o\&m} = C_{o\&m\text{-}WT} + C_{o\&m\text{-}PV} + C_{o\&m\text{-}ESS} \tag{10}$$

$$C_{cap\text{-}ESS} = \frac{1}{365}\left(c_1 CC_{cap\text{-}ESS} E_{ESS,max} \cdot y + c_2 CC_{cap\text{-}ESS} E_{ESS,max}\right) \tag{11}$$

$$y = \frac{r(1+r)^N}{(1+r)^N - 1} \tag{12}$$

$$r = \frac{r' - f}{1+f} \tag{13}$$

$$C_{rep\text{-}ESS} = \frac{1}{365}(n_{ESS} - 1) CC_{cap\text{-}ESS} E_{ESS,max} \tag{14}$$

Design2:

$$\min \ C_{o\&m} + C_{ng} \tag{15}$$

$$C_{o\&m} = C_{o\&m\text{-}WT} + C_{o\&m\text{-}PV} + C_{o\&m\text{-}GT} \tag{16}$$

$$C_{fuel} = C_{ng} F_{ng\text{-}total} \tag{17}$$

2.2.2. Constrains

(1) Output power from renewable energy generation

$$\beta \cdot P_{WT}(t) \le P_{WT\text{-}real}(t) \le P_{WT}(t) \tag{18}$$

$$\beta \cdot P_{PV}(t) \le P_{PV\text{-}real}(t) \le P_{PV}(t) \tag{19}$$

(2) ESS charge and discharge power

$$0 \le P_{ESS\text{-}charge}(t) \le P_{ESS\text{-}charge,max} \tag{20}$$

$$0 \le P_{ESS\text{-}disc}(t) \le P_{ESS\text{-}disc,max} \tag{21}$$

(3) ESS capacity

$$D_N E_{ESS,max} \le E_{ESS}(t) \le E_{ESS,max} \tag{22}$$

(4) Output power from gas turbine

$$0 \le P_{GT}(t) \le P_{GT\text{-}rated} \tag{23}$$

(5) Power balance

Design1:

$$P_{WT\text{-}real}(t) + P_{PV\text{-}real}(t) + P_{ESS\text{-}disc}(t) = \text{Load}(t) + P_{ESS\text{-}charge}(t) \tag{24}$$

Design2:

$$P_{WT\text{-}real}(t) + P_{PV\text{-}real}(t) + P_{GT}(t) = (1-\gamma)\text{Load}(t) \tag{25}$$

2.2.3. Evaluation criteria

In order to compare and analyze the cost of two different designs of microgrid, the Levelized Cost of electricity (LCOE) used in this paper. It is calculated by accounting for each part of cost incurred during the overall duration, including the cost of construction, financing, operation, maintenance, fuel, taxes, insurance and decommissioning, which are then divided by the total gross generation for the entire lifetime [18].

A simplified calculation method is applied in this paper, omitting the taxes, insurance and decommissioning, which is captured in (26) (27). nevertheless, the LCOE is still a useful way to compare the two different designs of microgrid.

$$LCOE = \frac{\sum_{n=1}^{N} \frac{C_{cap} + C_{O\&M} + C_{fuel}}{(1+r)^n}}{\sum_{n=1}^{N} \frac{P_{total,n}}{(1+r)^n}} \tag{26}$$

$$LCOEC = \frac{LCOE_{design_2} - LCOE_{design_1}}{LCOE_{design_2}} \tag{27}$$

3. CASE STUDY

3.1. Basic data

In order to verify the effectiveness of the proposed method, two different designs of small-scale microgrids with a 20-year lifetime are studied according to the methodology above in this section which contains renewable generating units (WT and PV) and ESS in the first design. Different from the first design is that we consider GTs rather ESS in the second design. The components of the microgrid systems are shown in Table 1.

Table 1 The components of the microgrid systems

Name	WT	PV	Design 1	Design 2
			Lead-acid Battery	GT
Type	30kW	0.2kWP	2V/1000Ah	\
Unit price	$100,000	2130 $/kW	$200	998 $*/kW
Source	[13]	[19]	[13]	[20]
Quantity	13	500	\	\

Capacity	390kW	100kW	\	\

* 6.8128 Yuan = 1 U.S dollar.

A typically day of transition season with 24 equal time slots is taken in account in this study. Similarly, the summer and winter case can be obtained easily according to the theory mentioned above. The Wind power, solar power and typical daily load is shown in Fig 3.

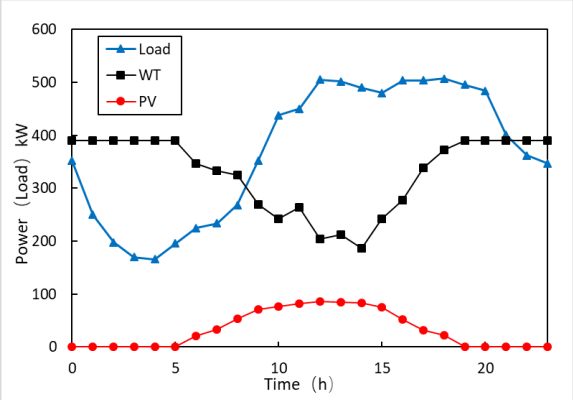

Fig 3 Wind power, solar power and typical daily load

We assume that the load is divided into important load and normal load and the normal load is all controllable. the controllable load is no more than 50% of the total load at any time [21]. Therefore, appropriate load reduction is clearly allowed in the second design in this paper, γ is set as 0-0.12 whose step length is 0.01.

Technical parameters of the WT are presented in Table 2.

Table 2 Technical parameters of the WT

Parameters	Values	Source
P_{rated}	30kW	[13]
V_{ci}	3 m/s	
V_{rated}	12 m/s	
V	24 m/s	

Other economic parameters are shown in table 3

Table 3 Economic parameters

Parameters	Values	Source
Annual inflation rate	2%	[1]
Nominal loan interest rate (Nominal discount rate)	8%	

The optimization problem can be written as a mixed integer linear programming (MILP) [21], which can be solved by IBM CPLEX12.8.0.

3.2. *Results and discussion*

3.2.1. *Comparison between design 1 and design 2*

Fig 4 and Fig 5 illustrate the variation of the LCOE versus the unmet load. The LCOE of the design 1 is 0.060$ in the first design when the DOD is equal to 80%, as illustrated in Fig 4. And in the second design, the LCOE varies from 0.064$/kWh to 0.056$/kWh as unmet load increases. Furthermore, we can see clearly that the LCOE of design 1 is lower when unmet load is greater than 0.06%. Otherwise, design 2 is better.

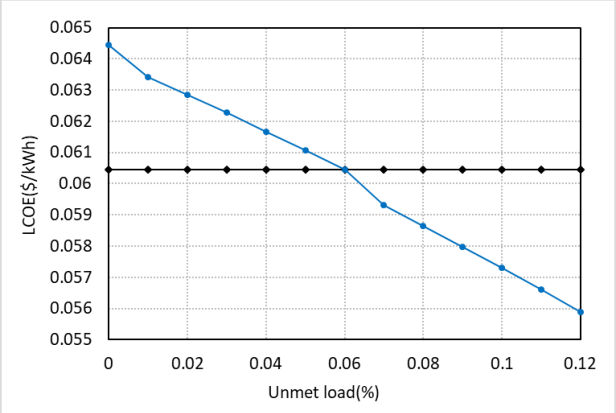

Fig 4 LCOE of design 1 and design 2

The cost difference is clearer which is illustrated in Fig 5. LCOE curtailment of design 2 is maximal when unmet load is equal to 0, which costs 6.23% lower than design1. The negative value of LCOE curtailment corresponds to the case where the cost advantages of design 2 decreases as unmet load increases. In other word, LOCE of design 1 is lower when unmet load is greater than 0.06.

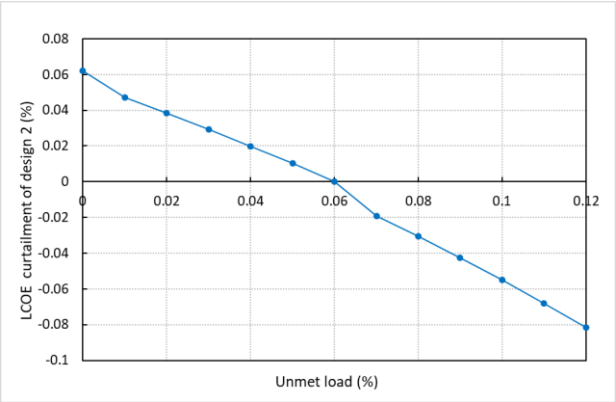

Fig 5 LCOE curtailment of design 2

3.2.2. *The effect of DOD of batteries to the optimal solution*

We now investigate the impacts of system parameter on comparative result. The variations in LCOE curtailment of design 2 with different values of the DOD are presented in

Fig. 6. As discussed above, the effect of discharge depth on battery cost is verified. As evident, LCOE curtailment of design 2 is reduced as DOD decreases. In other words, when DOD increases, the cost efficiency of design 2 is obvious. And when the DOD is lower than 0.6, no matter how the unmet load changes, design 1 is better.

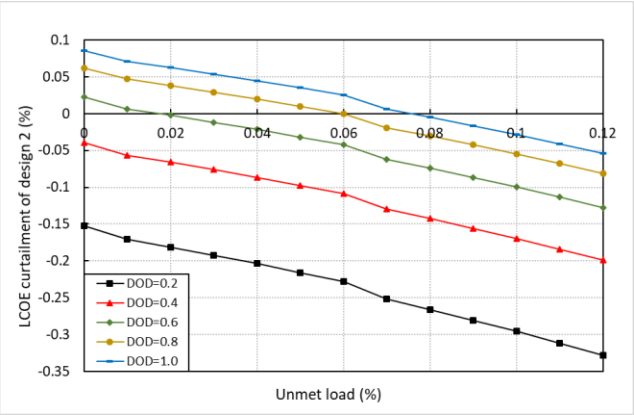

Fig 6 Impact of DOD of battery

3.2.3. The effect of renewable energy generation to the comparative result

To investigate the impact of the renewable energy penetration on the optimal solution, extra 5% and 10% renewable energy generation are added in this section. Here, we can see three scenes described in Fig 7 clearly. Overall, the impact of renewable power generation on LCOE curtailment is not obvious before 0.3. But after 0.3, this figure shows that higher amount of LCOE curtailment of design 2 can be achieved as the renewable energy generation and unmet load decreases.

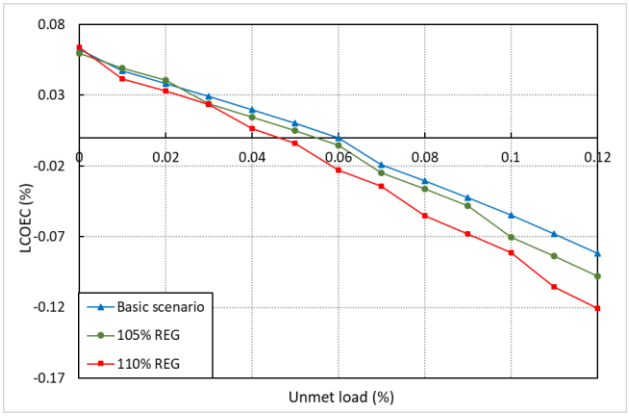

Fig 7 Impact of electricity production from renewable sources

4. CONCLUSION

We have proposed a contrastive framework for two different designs of microgrid with renewable energy considering battery lifetime and renewable energy penetration. Extensive numerical results have been presented to describe the LCOE curtailment of design 2 contrast with design 1. Based on the above work, we can draw the following conclusions.

(1) We propose a new scheme to optimize the cost of microgrid from the perspective of configuration strategy. The results prove that both designs we presented have their advantages in different situation.

(2) The impact of battery lifetime on costs cannot be ignored. Specifically, the LOCE curtailment of design 2 increases as DOD increases. In a brief, the large depth of discharge reduces the cost efficiency of the battery.

(3) The higher the renewable energy penetration is, the better the cost-effectiveness for design 1. Therefore, we can choose design 1 where renewable energy is abundant or GTs are operating where unmet load is equal to 0.

In order to obtain the optimal cost, two design modes of stand-alone microgrid are discussed in this study. In order to better show the proposed framework, grid-connected mode is also an area worth exploring. In addition, we assume that the generation of renewable energy units is deterministic. But in fact, the vagaries of the climate make renewable power generation volatile. Therefore, the influence of different design modes of microgrid on generation cost considering the uncertainty is also worth studying.

ACKNOWLEDGEMENT

The authors gratefully acknowledge the financial support provided by the National Natural Science Foundation of China under grant No. 71603039.

REFERENCE

[1] Palma-Behnke R, Benavides C, Lanas F, Severino B, Saez D. A Microgrid Energy Management System Based on the Rolling Horizon Strategy. IEEE Transactions on Smart Grid. 2013;4:996-1006.

[2] Shin'Ya O, Katsuaki S, Yuta U. Study on the operation optimization of an isolated island microgrid with renewable energy layout planning. Energy.

[3] Domenech B, Ranaboldo M, Ferrer-Martí L, Pastor R, Flynn D. Local and regional microgrid models to optimise the design of isolated electrification projects. Renewable Energy. 2018;119:795-808.

[4] Ghiasi M. Detailed study, multi-objective optimization, and design of an AC-DC smart microgrid with hybrid renewable energy resources. Energy. 2019;169:496-507.

[5] Razmi H, Doagou-Mojarrad H. Comparative assessment of two different modes multi-objective optimal power management of micro-grid: grid-connected and stand-alone. IET Renewable Power Generation. 2019;13:802-15.

[6] Alramlawi M, Gabash A, Mohagheghi E, Pu L. Optimal operation of hybrid PV-battery system considering grid scheduled blackouts and battery lifetime. Solar Energy. 2018;161:125-37.
[7] Li J, Xiong R, Mu H, Cornélusse B, Vanderbemden P, Ernst D, et al. Design and real-time test of a hybrid energy storage system in the microgrid with the benefit of improving the battery lifetime. Applied Energy. 2018;218:470-8.
[8] Dufo-López R, Lujano-Rojas JM, Bernal-Agustín JL. Comparison of different lead–acid battery lifetime prediction models for use in simulation of stand-alone photovoltaic systems. Applied Energy. 2014;115:242-53.
[9] Weitzel T, Schneider M, Glock CH, Löber F, Rinderknecht S. Operating a storage-augmented hybrid microgrid considering battery aging costs. Journal of Cleaner Production. 2018;188.
[10] Nguyen DT, Le LB. Optimal Bidding Strategy for Microgrids Considering Renewable Energy and Building Thermal Dynamics. IEEE Transactions on Smart Grid. 2014;5:1608-20.
[11] Borowy BS, Salameh ZM. Optimum photovoltaic array size for a hybrid/PV system. Energy Conversion IEEE Transactions on. 1994;9:482-8.
[12] Bo Z, Zhang X, Jian C, Wang C, Li G. Operation Optimization of Standalone Microgrids Considering Lifetime Characteristics of Battery Energy Storage System. IEEE Transactions on Sustainable Energy. 2013;4:934-43.
[13] Liu Z, Chen Y, Zhuo R, Jia H. Energy storage capacity optimization for autonomy microgrid considering CHP and EV scheduling. Applied Energy. 2018;210:1113-25.
[14] Faridoddin AS, Vladimir M. Novel performance curves to determine optimal operation of CCHP systems. Applied Energy.
[15] Zheng CY, Wu JY, Zhai XQ. A novel operation strategy for CCHP systems based on minimum distance. Applied Energy. 2014;128:325-35.
[16] Yang G, Zhai XQ. Optimal design and performance analysis of solar hybrid CCHP system considering influence of building type and climate condition. Energy. 2019;174:647-63.
[17] Nejabatkhah F. Optimal Design and Operation of a Remote Hybrid Microgrid. Cpss Transactions on Power Electronics & Applications. 2018;3:3-13.
[18] Gioutsos DM, Blok K, van Velzen L, Moorman S. Cost-optimal electricity systems with increasing renewable energy penetration for islands across the globe. Applied Energy. 2018;226:437-49.
[19] Gan Y, Zhai X. Optimization and performance analysis of solar hybrid CCHP systems under different operation strategies. Applied Thermal Engineering. 2018:S1359431117360635.
[20] Zhang T, Wang M, Wang P, Gu J, Zheng W, Dong Y. Bi-stage stochastic model for optimal capacity and electric cooling ratio of CCHPs—a case study for a hotel. Energy and Buildings. 2019;194:113-22.
[21] Shen J, Jiang C, Liu Y, Xu W. A Microgrid Energy Management System and Risk Management under an Electricity Market Environment. IEEE Access. 2016;4:2349-56.